Journal of Machine Engineering, 2018, Vol. 18, No. 2, 41-53
ISSN 1895-7595 (Print) ISSN 2391-8071 (Online)

Received: *05 January 2018* / Accepted: *20 April 2018* / Published online: *25 June 2018*

thermal effects, simulation, machine tool, environment, positioning errors

Janine GLAENZEL[1*]
Steffen IHLENFELDT[2]
Christian NAUMANN[1]
Matthias PUTZ[1]

EFFICIENT QUANTIFICATION OF FREE AND FORCED CONVECTION VIA THE DECOUPLING OF THERMO-MECHANICAL AND THERMO-FLUIDIC SIMULATIONS OF MACHINE TOOLS

Thermo-elastic deformations represent one of the main reasons for positioning errors in machine tools. Investigations of the thermo-mechanical behaviour of machine tools, especially during the design phase, rely mainly on thermo-elastic simulations. These require the knowledge of heat sources and sinks and assumptions on the heat dissipation via convection, conduction and radiation. Forced convection such as that caused by moving assemblies has both a large influence on the heat dissipation to the surrounding air. The most accurate way of taking convection into account is via computational fluid dynamics (CFD) simulations. These simulations compute heat transfer coefficients for every finite element on the machine tool surface, which can then be used as boundary conditions for accurate thermo-mechanical simulations. Transient thermo-mechanical simulations with moving assemblies thus require a CFD simulation during each time step, which is very time-consuming. This paper presents an alternative by using characteristic diagrams to interpolate the CFD simulations. The new method uses precomputed thermal coefficients of a small number of load cases as support points to estimate the convection of all relevant load cases (i.e. ambient conditions). It will be explained and demonstrated on a machine tool column.

1. INTRODUCTION

THERMAL EFFECTS are one of the main causes of positioning errors in machine tools; see Bonse et al. [1]. Next to friction and waste heat from the process and the drives, the heat dissipation to the environment has a large effect on the temperature distribution in a machine tool and consequently on its accuracy.

Heat is exchanged with the environment through conduction, free and forced convection and radiation. Among these, quantifying convection presents the greatest challenge because it dissipates large amounts of heat and it is difficult to simulate and even harder to measure. Simulations typically involve two steps. First computational fluid dynamics (CFD)

[1] Fraunhofer Institute for Machine Tools and Forming Technology IWU Chemnitz, Germany
[2] Dresden University of Technology, Institute of Machine Tools and Control Engineering, Dresden, Germany
[*] E-mail: Janine.Glaenzel@iwu.fraunhofer.de
DOI: 10.5604/01.3001.0012.0925

simulations are used to calculate the heat transfer coefficients on the machine tool surface. Then these coefficients are used as boundary conditions for thermal and thermo-mechanical simulations which determine the temperature and deformation fields of the machine tool. For transient thermo-mechanical simulations with moving assemblies, the convection heat transfer coefficients change during each time step due to the changes in speed and direction of the air flows surrounding the machine tool.

Accurate thermal simulations therefore require a new CFD simulation at almost every time step. This is more complicated by the fact that CFD simulations work with finite element (FE) discretizations of the surrounding air which need to be changed when the machine tool axis positions or the direction of the air flow changes. This presents a massive additional computational effort which is especially problematic for simulation based online TCP correction methods, such as the structure model based correction, see Kauschinger et al. [2].

In order to avoid complex CFD simulations, a commonly used alternative relies on empirical formulae [3] which describe the convection of simple geometrical bodies under specific presuppositions. Literature Drossel et al. [4] showed, however, that this simplification does not always achieve the accuracy needed to quantify thermo-mechanical effects. Despite this, current simulation based correction strategies (see Ess [5]) are forced to rely on these imprecise thermal coefficients to maintain real-time capability [6].

A solution to this dilemma which is based on the decoupling of CFD from thermo-elastic deformations using characteristic diagrams was first suggested in Glänzel et al. [7]. For this, the ambient conditions are quantified using the parameters air temperature, air speed and direction of air flow. Using these variables to describe individual ambient load cases, characteristic diagrams can be used to interpolate between these load cases. Thus a small number of training simulations can be used to establish a database from which a set of characteristic diagrams can accurately estimate, e.g., the heat transfer coefficients of all relevant ambient scenarios. After [7] had first introduced the idea and demonstrated its validity on a simple u-shaped geometry, Glänzel et al. [8] tested the idea on a stationary machine tool column with varying air temperatures and air speeds. This paper demonstrates that the proposed simulation decoupling strategy also works for changing directions of air flow. This seemingly small addition is particularly challenging because it requires new FE discretizations of the fluid surrounding the machine tool for each air direction and it completely changes the distribution of the heat transfer coefficient amplitudes across all machine surfaces which significantly complicates their interpolation. The ability to also interpolate different directions of air flow presents the missing key needed to incorporate forced convection of moving assemblies into the characteristic diagrams and thus complete the decoupling approach.

The different steps required for the decoupling of CFD from thermo-mechanical simulations will be described the next chapter. It relies largely on clustering algorithms and characteristic diagram interpolation which are explained in more detail in Chapters 3 and 4 respectively. Chapter 5 will then present the numerical calculations that were done to demonstrate the decoupling approach on a machine tool column under changing ambient conditions. Chapter 6 will conclude with a summary and an outlook on further research.

2. PROCEDURE FOR SIMULATION DECOUPLING

To study the interactions between the machine tool and its environment, fluid-structure-mechanical simulations have to be performed. Such coupled fluid-structure-mechanical simulations are very performance intensive, particularly if many different ambient load scenarios are possible during production. In preparation for the decoupling of the fluid and thermo-elastic simulation through characteristic diagrams, the relevant parameters (e.g. temperature, heat transfer coefficients (HTC), heat flux, flow velocity, flow direction) obtained from CFD simulations have to be exported. These characteristic diagrams act as boundary conditions for the thermo-elastic simulation in order to include the heat exchange with the environment.

Before the determined ambient parameters can be used for the characteristic diagram interpolation, a reduction of the large amount of geometry nodes (finite element nodes) is required. The ambient parameters vary for each node of the surface FE mesh of the machine tool. The nodes of the surface FE mesh in the output *.csv file from ANSYS act as sample points for generating the Radial Basis Function (RBF) interpolation (see Buhmann [9], Unger [10]). For the interpolation, polyharmonic spline RBFs are chosen. The main advantages of the use of this RBF approach for the decoupling are:

- Remeshing of the FE data for post processing through RBFs;
- Support for the optimization of characteristic diagram grids;
- Better handling of big data and high number of degrees of freedom through selective filtering of relevant data;
- Characteristic diagrams could be computed for each RBF node.

This leads to an adequate clustering of ambient parameters, so that more values are chosen in areas with big changes, e.g. along the edges, and fewer are placed in areas with small changes, e.g. nearly constant areas. Calculating characteristic diagrams for the RBF nodes would eliminate the need to include the geometric grid of the machine tool surfaces in the characteristic diagram grid. This would make coordinate transformations (see Chapter 5) unnecessary and reduce the grid size significantly. However, this will only work, if the RBF clustering is independent of the ambient load case, including the direction of air flow. The other disadvantage would be that the RBF approximation error would be added to that of the characteristic diagram interpolation. Through RBF interpolation, the necessary ambient values can be clustered and used as input parameters for characteristic diagrams. The next step in our research enables the clustering of complex geometries via the development of an optimization algorithm for optimal clustering. This algorithm will automatically select the best or optimal subset of all RBF functions.

3. CLUSTERING OF HEAT TRANSFER COEFFICIENTS BY OPTIMAL SUBSET PROBLEM

The CFD simulation in ANSYS computes the heat transfer coefficients (HTC), velocity vectors or other ambient parameters in a huge number of nodes on the surface of the computed

domain. Because of the very large number of nodes, it is desirable for fast evaluations to reduce this number of nodes while maintaining the accuracy. This is done by choosing a 'good subset' with a fixed size m of node number values which will be used to build an interpolation function, based on radial basis functions. The mathematical formulation for choosing these optimal nodes for the interpolation can be done in the following way.

Given a set $V = \{1, 2, \cdots N\}$ which corresponds to the nodes $x_1, x_2, \cdots, x_N$ of the FE simulation and their computed HTC values $w_1, w_2, \cdots, w_N$. Furthermore, define a number m < N and a weighting function

$$\xi : S \subset V \to \mathbb{R}_0^+ \quad \text{with} \quad |S| = m \tag{1}$$

which maps an m-sized subset S to a real number greater or equal zero. Consequently, the „Optimal Subset Problem" becomes the minimization of this weighting function ξ as

$$\begin{array}{l} \min \quad \xi(S) \\ S \subset V, \\ |S| = m \end{array} \tag{2}$$

In our application, the weighting function ξ is a function calculating the interpolation error which occurs when the m node values of S are used to build the radial basis interpolation function f_S like in Glänzel et al. [11], evaluate it in all N nodes of the set V and compare the interpolated values with the given values w_i. Possible error measures are the sum of squares

$$\xi(S) := \sqrt{\sum_{i=1}^{N} (f_S(x_i) - w_i)^2} \tag{3}$$

or a pointwise computed maximum error

$$\xi(S) := \max_{i=1\cdots N} |f_S(x_i) - w_i)| \tag{4}$$

Clearly the value of $\xi(S)$ is (aside from small rounding errors) zero if $m = N$, that is $S = V$, but it becomes greater than zero for $m < N$.

The challenge now is to find the optimal subset S that leads to the minimum of weighting function ξ. For very small sets V and small numbers m this can be done by computing all possible subsets $S \subset V$ and compare the values of ξ, but in all practically relevant cases this becomes impossible due to the combinatorial explosion. The number of different subsets $S \subset V$ of size m is given by the binomial coefficient N over m.

The minimization of a function ξ is a widely used technique for solving optimization problems. Depending on the properties of the function which is to be minimized (continuity, differentiability, ...) many effective algorithms exist for such classes of functions. Nevertheless, the challenge of our minimization problem eq. (2) is that our weighting function ξ is not continuous. Moreover, it is defined over a discrete set. All algorithms depending on

gradients are not applicable for such a problem. However, there exists one widely used technique for such problems, which is the class of genetic algorithms. The basic idea of these algorithms is to duplicate the selection of the fittest in natural evolution processes. A solution candidate is seen as an individual, a bulk of individuals is seen as population and the population is developed from one generation to the next generation by annihilating individuals with poor fitness, selecting individuals with good fitness for reproduction and creates a new generation in Glänzel et al. [11]. This optimized RBF clustering technique was used here for the reduction of the characteristic grid size, see Chapter 5.

4. CHARACTERISTIC DIAGRAM BASED INTERPOLATION

Characteristic diagrams are a fundamental tool of engineers used to approximate real-valued functions that depend on one or more input variables. The characteristic diagrams used in this paper are based on the smoothed grid regression introduced by Priber in 2003 [12] and later improved to enable efficient, high-dimensional characteristic diagrams able to approximate thermo-elastic deformations in machine tools (see Ihlenfeldt et al. [13]). These characteristic diagrams comprise a rectangular grid of support points and a set of kernel functions used to interpolate between them. Popular kernels are polynomials or splines, where higher-dimensional kernels are usually created by multiplying one-dimensional kernels (see Priber [12]).

The creation of a characteristic diagram starts with the selection of input variables needed to approximate the output variable. It is usually of vital importance to include all relevant input variables. A good characteristic diagram algorithm will however not mind the inclusion of unnecessary additional variables so long as the total grid size remains manageable. An example of this might the integration of air pressure or humidity into the calculation of the heat transfer coefficient. Both parameters have been ignored in this paper because their expected range has very little impact on the HTCs. The next step is to define and discretize the domain of each variable where the fineness of the discretization depends on the variability of the directional derivative and the type of kernel used. The type of kernel is thus usually chosen along with the grid fineness in order to obtain optimal grids and avoid overfitting. Given a sufficiently fine grid, simple piecewise multilinear kernels are sufficiently accurate and generally well suited for the approximation of thermal deformations in Ihlenfeldt et al. [13]. While complex grid structures may sometimes be useful in minimizing the necessary degrees of freedom of a characteristic diagram, simple equidistant grids often perform equally well and are best at avoiding overfitting in thermal error estimation in Glänzel et al. [14]. The next step is the gathering of training data which comprises a set of input data and their corresponding output data. These may be obtained from measurements or simulations and should cover as much of the input domain as possible. From this training data, data fitting equations are created in a least-squares error minimization approach. Since the data is most often sparse in comparison to the rather large grids, the assumption of smoothness is used to turn the underdetermined system into an overdetermined system by adding smoothing equations.

The resulting linear system then provides the coefficients of the kernel functions for each grid vertex and thereby defines the characteristic diagram. A detailed account of the entire algorithm can be found in Priber [9] and Naumann et al. [15]. In Herzog et al. [16], a new finite element method (FEM) based algorithm is described and tested which permits a more efficient computation of characteristic diagrams using multigrid solvers and thereby enables characteristic diagrams with ten or more input variables.

One possible application of characteristic diagram based interpolation is the estimation of thermal deformations from a small set of temperature sensors (strategically distributed across the machine tool surface) and the axis positions, which has been thoroughly investigated and tested in [13-16]. Another application is the approximation of heat transfer coefficients for the accurate modelling of the heat dissipation through convection in thermal simulations of machine tools. As previously stated, the first step is to select the necessary input variables. The convection heat transfer coefficient (HTC) α depends mostly on the type of fluid (here: air), its temperature and in the case of forced convection the speed and direction from which the fluid streams against the surface (see Cengel [17]). For free convection, the shape and orientation of the surface is also very important but this is implicitly taken into account. Therefore the characteristic diagram should approximate the following mapping:

$$\alpha = f(x, y, z, \vec{v}_{air}, T_{air}), \tag{5}$$

for all points (x, y, z) on the machine tool surface. On smooth surfaces, the convection heat transfer coefficient is likewise smooth and continuous. On the edges between machine faces, however, the HTC will often jump abruptly. Therefore, characteristic diagram interpolation may only be used if each machine face is considered separately. For air flow and temperature, simple equidistant grids with multilinear kernel functions should be well suited for HTC interpolation. As the preliminary investigations on HTC interpolation (see Glänzel et al. [7, 8]) have shown, discretization fineness can be very coarse for the air temperature and less coarse for the air speed. Chapter 5 will show that the direction of the air flow will need to be finely discretized in order to achieve accurate approximations of the HTC. It will also be shown, that the variation of the direction of the air flow requires a much finer geometic discretization of the machine tool surface than before (see Glänzel et al. [8]). For practical reasons it is recommended to transform all machine faces to 2D surfaces in Glänzel et al. [8]. This reduces the grid size while at same time improving the quality of HTC approximation.

Since measuring the HTC across the entire machine tool surface is next to impossible, the training data must be created by CFD simulations. For this, ideally one simulation should be done for each grid vertex (ignoring the geometric dimensions), i.e.

$$(\vec{v}_{air}, T_{air}) = (v_{azimuth}, v_{elevation}, |v|, T_{air}) \in \Re^4, \tag{6}$$

where the air flow is expressed in polar coordinates with the radius being the air speed. A sample discretization might then be:

$$v_{azimuth} \in \{0°, 45°, 90°, 135°, 180°, 225°, 270°, 315°\},$$

$$v_{elevation} \in \{-90°, -45°, 0°, 45°, 90°\},$$

$$|v| \in \{0, 3, 6, 9\} \left[\frac{m}{s}\right],$$

$$T_{air} \in \{10°, 35°\}.$$

This (realistic) discretization would require 8·3·3·2 + 2·3·2 + 2 = 158 CFD simulations to acquire the necessary training data for the interpolation of all relevant ambient conditions.

5. CASE STUDY – MACHINE TOOL COLUMN

The idea of the decoupling of CFD from thermal simulations is to perform a relatively small number of CFD simulations once prior to any thermal simulations, then compute a set of characteristic diagrams from them and finally to be able to use these characteristic diagrams to obtain accurate boundary conditions for thermal simulations for all relevant ambient scenarios. To verify this idea, one must choose a sufficiently complex sample geometry, perform enough CFD simulations for the computation of the needed characteristic diagrams and then test the interpolation of ambient load cases using further test CFD simulations that were not used in the training of the characteristic diagrams. Using the training and test error provided by the characteristic diagrams, one must then choose a meaningful error measure to evaluate the quality of the interpolation. The decoupling would fail if singularities occurred, i.e. if some small change in any of the input variables caused very large local changes in the HTCs and would thus make characteristic diagram interpolation impossible. It might also be considered a failure if the resulting algorithm becomes more computationally complex than the coupled simulation.

The geometry chosen for this investigation was the machine tool column of the ACW 630 made by Auerbach, a three-axis milling machine of the Chemnitz University of Technology. A CAD model the ACW630 can be seen in Fig. 1 where the greyed-out sections were ignored in the simulations. It is one of the demonstration machines in the project CRC/TR96 which was chosen because several thermal and ambient measurements scheduled for 2018 will provide the experimental validation for the performed simulations. With its roughly 900 surfaces discretized into almost 150,000 finite elements, it is certainly sufficiently complex for this demonstration.

The interpolation of the convection heat transfer coefficients (HTCs) needs to be demonstrated for all of the dependent variables, i.e. the direction and speed of the air flow, the ambient temperature and the geometric location on the machine tool surface. The interpolation of air speed, ambient temperature and geometric location were tested in [8]. It was shown that all three variables can be interpolated using characteristic diagrams and the interpolation error, even for relatively coarse grids, was still well below 5% and could easily be improved with more training simulations and finer discretizations. What remains, is

showing that the interpolation of different directions of air flow is likewise possible. This is, however, much more difficult because unlike the previous investigations, changing the direction of the air flow will not only change the magnitude of the HTCs but also their distribution across the machine tool surface. Apart from the more complex interpolation, the clustering of the HTCs becomes far more difficult and the bounding fluid volume needs to be remeshed for every change in the direction of the air flow.

Fig. 1. Machine tool column of the ACW-630

The interpolation of the convection heat transfer coefficients (HTCs) needs to be demonstrated for all of the dependent variables, i.e. the direction and speed of the air flow, the ambient temperature and the geometric location on the machine tool surface. The interpolation of air speed, ambient temperature and geometric location were tested in [8]. It was shown that all three variables can be interpolated using characteristic diagrams and the interpolation error, even for relatively coarse grids, was still well below 5% and could easily be improved with more training simulations and finer discretizations. What remains, is showing that the interpolation of different directions of air flow is likewise possible. This is, however, much more difficult because unlike the previous investigations, changing the direction of the air flow will not only change the magnitude of the HTCs but also their distribution across the machine tool surface. Apart from the more complex interpolation, the clustering of the HTCs becomes far more difficult and the bounding fluid volume needs to be remeshed for every change in the direction of the air flow.

As is explained in Chapter 4, the interpolation of the geometric location is only possible for individual machine faces, in order to guarantee continuous and smooth HTCs across the entire grid. Based on the given FE mesh of the machine tool, [8] explains the necessary steps to deal with this issue and obtain a set of minimal characteristic diagrams for the entire geometry.

1. Assign all finite elements to machine faces. Machine faces are all connected, smooth, continuous surfaces of the machine tool. They are usually, if not necessarily, flat. Typically this assignment can be obtained from the simulation software.

2. Define characteristic diagrams for each machine face (input variables, grid discretization).
3. Reduce size of characteristic diagrams using error estimators. Particularly for very small or less exposed surfaces, simpler characteristic diagrams will suffice. This usually means leaving out one or more of the input variables. Using the training data, one can compute all characteristic diagrams and coarsen or refine depending on the approximation error.
4. Transform all machine faces into 2D and rotate them to obtain a minimal 2D bounding box. Depending on the size and curvature of the face, Glänzel et al. [8] suggests and compares several algorithms to do so. Since most faces are already flat, projections are usually best. The new and transformed 2D coordinates of all FE nodes are stored so that these transformations need only be done once.
5. Computation of the coefficients of the characteristic diagrams for all machine surfaces using the simulated training data.

The biggest advantages of characteristic diagrams are their simplicity and their versatility. In this case, this means that the addition of the direction of air flow, represented by the two new input variables $v_{azimuth}$ and $v_{elevation}$, requires no significant adjustments of the interpolation. However, some other aspects of the algorithm still needed to be changed. Since the distribution of the HTCs across the machine tool surface changes with the direction of the air flow, the clustering needs to be altered to take this into account. Since this problem has not yet been solved, the clustering algorithm from chapter 3 was once again used here. After the clustering of HTCs on each machine surface, the optimized RBFs were tested on all training data simulations. Where the RBF interpolation error was below a set threshold, the clustering was considered successful and the clustered RBFs were used to optimize the geometric grid of the characteristic diagrams. This means that the locations of the optimized RBFs on the machine tool surface were used to find better support points for variable grids, see Glänzel et al. [8, 14]. Since the HTCs were previously transformed into 2D, the RBF clustering becomes relatively simple and their optimized positions are already in the target 2D coordinates. Where clustering was unsuccessful, equidistant grids with a much finer discretization were used to map the changing distributions of the HTCs. One such face, where load case independent RBF clustering was not possible can be seen in Fig. 2, portraying the left side face of the column with the air flow streaming from two different angles about 45° apart.

To quantify the interpolation error, the difference in heat dissipation per 1K temperature difference integrated across the entire surface of the machine tool column was used. Heat dissipation $\dot{Q}$ is given by $\dot{Q} = \alpha A \Delta T$.

The proposed error measure with the true HTC α and the approximated HTC $\tilde{\alpha}$ is thus

$$\int_A \Delta\dot{Q}(x,y) \Big/ \Delta T \, dxdy = \sum_{i \in FE} (\tilde{\alpha}_i - \alpha_i) A_i. \tag{7}$$

This error measure was used in the evaluation of the characteristic diagram based interpolation. For the reduction of the grid size (step 3), this error measure was used to find the smallest grid that still produced a heat dissipation error below a set threshold. Finally,

the error measure was also used to evaluate the fitting of the test data and verify the proposed decoupling method.

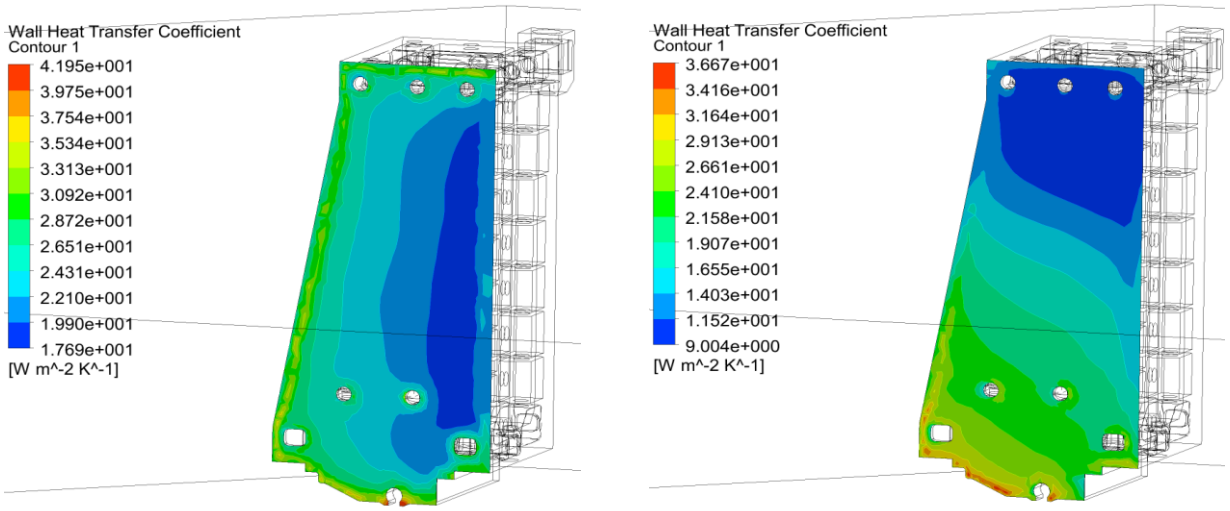

Fig. 2. Wall HTCs of the left face of the machine tool column for forced convection with direction of air flow (45°, 0°) (left) and (45°, 45°) (right)

From the multitude of CFD simulations performed for this investigation only three will be used for this simple verification of the decoupling approach. Thermal simulations are not necessary at this point because the temperature of the solid (machine tool) does not affect the HTCs and is thus not relevant for the decoupling itself. To simulate different directions of air flow, which was the main focus of the paper, a convex hull shaped like a circus tent was placed around the machine tool column, see Fig. 3.

Figure 3 shows the convex hull of the surrounding air along with the inlets and outlets used for one of the CFD simulations for the training data. The other training load case used the yellow-tinged face in the front as inlet. The load case used to test the interpolation used the red-rimed face between the two previous faces as inlet. This creates a very coarse grid for $v_{azimuth}$ (of 90° steps instead of the suggested 45°) and ignores $v_{elevation}$ altogether. Since there are roughly 900 individual faces on the column with many different face normals, it is not necessary to test the interpolation from every direction of $v_{azimuth}$ and $v_{elevation}$, because one can assume that every combination of face normal and air direction are represented in the scenario. Since the interpolation needs to work on every face, the maximum relative interpolation error needs to be checked to determine the success of the interpolation. Relative error in this case means that the error in heat dissipation of each face must be divided by the actual amount of heat dissipated across that surface for the selected load case. This procedure is essentially the same as for determining which input variables can be omitted and how fine the discretization needs to be, which are done during the grid reduction (step 3).

Table 1 shows the results of both parts of the verification of the decoupling approach. The first part (see Glänzel et al. [8]) omitted the direction of the air flow and was thus far simpler and more accurate.

The second part investigated for this paper did not achieve the same level of accuracy because of the relatively small number of simulations used to train the characteristic diagrams. The results can be considered a simple proof-of-concept. Characteristic diagrams can therefore be used to interpolate HTCs for free and forced convection using the methods described above and in Glänzel et al. [8]. The effort to realize the decoupling of CFD from thermal simulations lies mainly in the grid transformation (see steps 1-4 above) and the reduction of the resulting characteristic diagrams. If memory is not an issue, then the reduction step can be omitted. This would not affect the computation time significantly when used within thermal simulations.

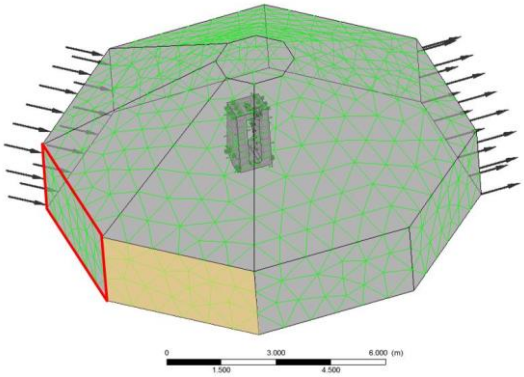

Fig. 3. Convex hull of air around machine tool column with inlets and outlets

Table 1. Two parts of decoupling method verification

Method verification	1 [8]	2
Full char. diagram grid	$(\tilde{x}, \tilde{y}, \lvert v \rvert, T_{air}) \in \Re^4$	$(\tilde{x}, \tilde{y}, v_{azimuth}, v_{elevation}, \lvert v \rvert, T_{air}) \in \Re^6$
N° simulations required	≥ 8	≥ 320
HTC RBF clustering	unrestricted	only for few faces, after verification
Relative error of test case	1.4 %	11.4 %
Estimated memory Requirement for char. diagram interpolation	(19,832 + 2·69,764)·4B = 637.4 KB	< (8·5·19,832 + 2·69,764)·4B = 3,731.2 KB

Using this extended methodology of HTC approximation with expanded characteristic diagram grids, conditional clustering and a set of additional CFD simulations with changing directions of forced convection, HTC approximation was once again verified and the results compared to the initial investigation (detailed in Glänzel et al. [8]).

5. SUMMARY, CONCLUSION AND OUTLOOK

Accurate thermal simulations require the precise knowledge of the ambient conditions in order to correctly consider the heat dissipation to the environment. One important aspect of this is the knowledge of the convection heat transfer coefficient (HTC) for free and forced convection between the machine tool and the surrounding air. HTCs taken from fixed tables or computed from empirical formulae are often not sufficiently accurate, so that

computational fluid dynamics (CFD) simulations are the only way to obtain accurate HTCs. If the ambient conditions change or certain assemblies of the machine tool move at varying speeds, then the HTCs also change requiring coupled CFD and thermal simulations.

The paper presents a new method aimed at decoupling the CFD from the thermal simulations using characteristic diagrams to interpolate HTCs between known ambient load cases. Based on a set of apriori simulated ambient load cases which coarsely cover the all possible ambient conditions, characteristic diagrams provide a means of instantly providing precise HTCs for every ambient scenario. This method was previously developed and tested without considering changing directions of air flow. This paper demonstrates that the decoupling works even under changing directions of air flow and explains the necessary adaptions needed to make it work. The main differences in the decoupling method are that two additional input variables are added to the characteristic diagrams to account for the global direction of the air flow and that the optimization of the geometric grid using clustering has to be tested for each machine face and replaced by fine equidistant grids where clustering fails. For the verification three different directions of air inlets, each 45° apart were used to test the interpolation. The required CFD simulations were done using a multi-faceted convex hull able to represent various different directions of air flow.

The conclusion of this investigation in combination with the previous study is that the new decoupling method works, provided the discretization of the input variables is sufficiently fine. This means, that a relatively large number of CFD simulations (e.g. 320) are required to gather the necessary training data for the characteristic diagrams and that with one characteristic diagram per machine face, the necessary memory to store the grids and coefficients also becomes large (several MB). Despite this, the time it takes to compute the HTCs from the many characteristic diagrams for a given ambient load case is still negligible.

Further investigations into the decoupling will be focused on the coupling of the characteristic diagrams of the HTCs with the thermal simulations. Algorithms for the automatic integration of the characteristic diagrams into transient thermo-elastic simulations are currently being developed and implemented. Here it was assumed that the air flows globally from a single direction against the machine tool. For moving assemblies there is no such global air flow but rather each assembly experiences a local air flow depending on its speed and direction of movement. Thus at any given time, each assembly might have a different ambient load case so that different sets of HTCs need to be combined automatically. In addition a truly coupled simulation will be set up to validate this method and provide a comparison in terms of setup effort and computational effort. The new method will also be compared to HTCs computed from state-of-the-art empirical formulae to demonstrate the improvements in accuracy. A modified version of the RBF clustering is also being developed to account for the changing distributions of HTCs under varying directions of air flow.

ACKNOWLEDGMENTS

This research was supported by a German Research Foundation (DFG) grant within the Collaborative Research Centers/Transregio 96, which is gratefully acknowledged.

REFERENCES

[1] WECK M., MCKEOWN P., BONSE R., HERBST U., 1995, *Reduction and compensation of thermal errors in machine tools*, Annals of the CIRP, 44/2, 589-598.
[2] KAUSCHINGER B., MÜLLER J., RIEDEL M., THIEM X., 2016, *Principle and verification of a structure model based correction approach*, Procedia CIRP 46, 111-114, DOI: 10.1016/j.procir.2016.03.169.
[3] Verein Deutscher Ingenieure (VDI), 2006, *VDI-Wärmeatlas – Berechnungsblätter für den Wärmeübertrag*. VDI Verlag Berlin.
[4] DROSSEL W.G., GROSSMANN K., IHLENFELDT S., SCHROEDER S., ZWINGENBERGER C., 2013, *Modellierung des Wärmeaustauschs Maschine-Umgebung*, Tradition und Gegenwart bei der Analyse des thermischen Verhaltens spanender Werkzeugmaschinen, 16, Dresdner Werkzeugmaschinen-Fachseminar.
[5] ESS M., 2012, *Simulation and Compensation of Thermal Errors of Machine Tools*, Dissertation, ETH Zurich.
[6] GLÄNZEL J., IHLENFELDT S., NEUGEBAUER R., RICHTER C., ZWINGENBERGER C., 2015, *Modelling of thermal interactions between environment and machine tool*, Thermo-energetic Design of Machine Tools, Lecture Notes in Production Engineering, Springer, 111-124.
[7] GLÄNZEL J., IHLENFELDT S., NAUMANN C., PUTZ M., 2016, *Decoupling of fluid and thermo-elastic simulations of machine tools using characteristic diagrams*, Proceedings CIRP ICME 2016, Ischia (Italy).
[8] GLÄNZEL J., IHLENFELDT S., NAUMANN C., 2017, *Effiziente Quantifizierung der Konvektion durch Entkoppelte Strömungs- und Strukturmechanische Simulation, Beispielhaft am Maschinenständer*, 5 Kolloquium SFB/TR96, Chemnitz.
[9] BUHMANN M.D., 2004, *Radial Basis Functions*, Cambridge University Press.
[10] UNGER R., 2009, *Obstacle Description with Radial Basis Functions for Contact Problems in Elasticity*, Preprint CSC 09-01 TU Chemnitz.
[11] GLÄNZEL J., UNGER R, IHLENFELDT, 2018, *Clustering by optimal subsets to describe environment interdependencies*, Conference on Thermal Issues in Machine Tools, Dresden.
[12] PRIBER U., 2003, *Smoothed Grid Regression*, Proceedings Workshop Fuzzy Systems, Vol. 13, Dortmund, Germany, 159-172.
[13] IHLENFELDT S., NAUMANN C., PRIBER U., RIEDEL I., 2015, *Characteristic Diagram Based Correction Algorithms for the Thermo-elastic Deformation of Machine Tools*, Proceedings 48th CIRP CMS, Naples.
[14] GLAENZEL J., IHLENFELDT S., NAUMANN C., PUTZ M., 2017, *Optimized Grid Structures for the Characteristic Diagram Based Estimation of Thermo-elastic Tool Center Point Displacements in Machine Tools*, Journal of Machine Engineering, 17/3.
[15] NAUMANN C., PRIBER U., 2012, *Modellierung des Thermo-Elastischen Verhaltens von Werkzeugmaschinen mittels Hochdimensionaler Kennfelder*, Proceedings Workshop Computational Intelligence, Dortmund, Germany.
[16] HERZOG R., NAUMANN C., PRIBER U., RIEDEL I., 2015, *Correction Algorithms and High-Dimensional Characteristic Diagrams*. In: Thermo-energetic Design of Machine Tools, Lecture Notes in Production Engineering, Springer, 159-174.
[17] CENGEL Y.A., 2003. *Heat Transfer: A Practical Approach*. McGraw-Hill, 2nd Edition.